ESR study of photoinduced defects in isotopically enriched quasi-one-dimensional chlorine-bridged platinum complexes

X. Wei, S. R. Johnson, B. I. Swanson, and R. J. Donohoe*
CST-4, MS J586, Los Alamos National Laboratory, Los Alamos, New Mexico 87545
(Received 27 January 1997)

Photoinduced defects in the quasi-one-dimensional chlorine-bridged platinum complex, $[Pt^{II}(en)_2][Pt^{IV}(en)_2Cl_2](ClO_4)_4$, where en=ethylenediamine, $C_2N_2H_8$, were investigated by light-induced electron-spin resonance (LESR). Using samples prepared with enriched nuclear isotopes including ^{194}Pt ($I=0$), ^{2}H ($I=1$), and ^{37}Cl ($I=3/2$, magnetogyric ratio $\sim$83% that of ^{35}Cl), the hyperfine and superhyperfine (SHF) patterns in the LESR spectra were fully characterized. The SHF structure (16 G average spacing) is unequivocally assigned to the bridging chlorines by comparison of the LESR spectra from samples with natural abundance Cl with samples enriched with ^{37}Cl. The LESR spectra were analyzed at $g_\perp$, $g_\parallel$, and intermediate angles by simulation of both the polaron and soliton-spin distributions. The results at temperatures above 6 K were found to be in better agreement with the neutral soliton assignment advanced by Kuroda and co-workers. The spectra from 6 to 140 K do not indicate motional narrowing as has been previously suggested. Below 6 K, surprisingly, the LESR spectra of both the natural and isotopically enriched samples exhibit an unusual dependence on temperature, modulation frequency, or microwave power, which indicates the presence of a localized dynamic process. Two other types of defect which exhibit strong sample-to-sample variability were also discovered in the LESR spectra: one is likely a spin triplet, and the other appears only at temperatures above approximately 120 K and is quite intense and stable at room temperature. [S0163-1829(97)03037-3]

I. INTRODUCTION

Intrinsic and photoinduced excitations in quasi-one-dimensional halide-bridged mixed-valence metal complexes (M-X) have been the subject of significant interest.[1–9] These linear chains have been synthesized with a variety of metals (Pt, Pd, and Ni), halogens (I, Br, Cl), equatorial ligands and counterions. While the average oxidation state of the metals in an M-X chain is $+3$, this structure is unstable to a Peierls distortion: the strong electron-electron and electron-lattice interactions lead to charge disproportionation between the metals (alternating sites tending toward $+4$ and $+2$ valences) and dimerization of the halide sublattice toward the higher valence metal sites, as illustrated in Fig. 1. As a result, a commensurate charge-density-wave (CDW) ground state is formed with the degree of charge disproportionation (strength of CDW) dependent upon all aspects of the chemical makeup and also upon environmental influences such as temperature and pressure. $[Pt^{II}(en)_2][Pt^{IV}(en)_2Cl_2](ClO_4)_4$ (where en=ethylenediamine, $C_2N_2H_8$), referred to hereafter as Pt-Cl, is a well-known example of these complexes.[8,9] For a given composition of equatorial ligands and counterions, the strength of the CDW increases in the series Ni<Pd<Pt and I<Br<Cl, making Pt-Cl chains strong CDW materials.

Much of the interest in MX complexes is generated by the fact that they can serve as a well controlled experimental testing ground for the examination of highly correlated narrow-band electronic materials, including the low-dimensional elements of high-temperature superconductors (Cu-O planes and chains). Mishima and Nasu[8] have developed a half-filled, one-band Peierls Hubbard model in which only the metal electronic structure is explicitly included whereas Gammel *et al.*[9] have developed a three-quarter-filled, two-band model where both halide and metal electronic structures are included. Both approaches have enjoyed considerable success in modeling the CDW ground state and various localized excited states, such as spin-1/2 polarons and neutral solitons, and spinless bipolarons, charged solitons and excitons.

While both polaron and soliton excitations (see Fig. 1) have been suggested to coexist in Pt-Br and Pt-I complexes,[3] the nature of photoexcitations in Pt-Cl has been the subject of controversy. In their original study of the electron-spin-resonance (ESR) spectrum of Pt-Cl, Kawamori, Aoki, and Yamashita[7] observed a signal at $g_\perp \approx 2.3$ which exhibited a five-line hyperfine (HF) structure with approximately 180 G splitting and intensity ratio of 1:8:18:8:1. Later, light-

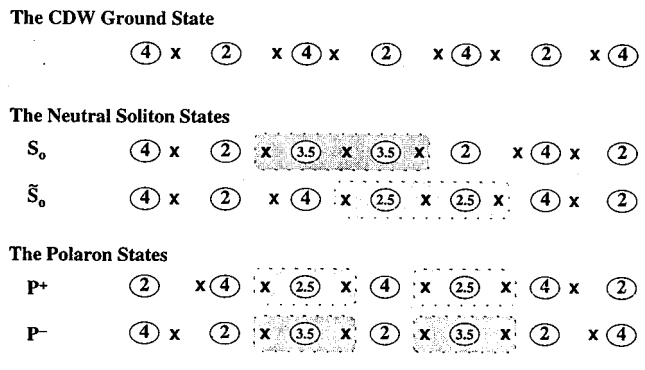

FIG. 1. A schematic diagram of Pt-Cl in its ground state and polaron as well as soliton excitations, where × denotes Cl^-, the numbered ovals denote Pt sites with the number representing the approximate oxidation state, and the hatched pattern represents a spin distribution.

induced ESR (LESR) studies showed that this signal can be photogenerated and is correlated with photoinduced absorption and Raman features in Pt-Cl.[10–16] The signal was first assigned to spin-1/2 neutral solitons localized on two equivalent Pt sites. The HF intensity pattern was attributed to the probability of finding the total nuclear-spin moment I_z of the two Pt at -1, $-1/2$, 0, 1/2, and 1, which yields the observed result because natural Pt consists of 33.7% ^{195}Pt with nuclear spin-1/2 and 66.3% Pt isotopes with no nuclear spin.

While the general features of the $g_\perp$ spectrum have been reasonably assigned, there have been a variety of inconsistencies in the LESR data. First, the published $g_\parallel$ spectra have not always been identical (cf. $g_\parallel$ in Refs. 7 and 11), suggesting that sample and/or experimental variations are significant. Second, the 16-G-spaced superhyperfine (SHF) structure has not always been observed for the $g_\perp$ signal. Kawamori and co-workers observed this structure in their original study and tentatively attributed it to interactions of the unpaired electron spin with the nitrogens on the equatorial en ligand. However, a later report[13] from our laboratory demonstrated that this could not be the case because synthesis of Pt-Cl with ^{15}N-labeled en ligands was shown to have no effect upon this structure, and we suggested that the SHF on $g_\perp$ was due to bridging chlorines.

Apart from the experimental results, there has been a fundamental disagreement regarding the nature of the defect associated with the LESR spectrum in particular and the photoinduced spectroscopic signals (including absorption[17,18] and resonance Raman[19]) in general. Both polaron and soliton descriptions have been advanced, and theoretical descriptions of both types of defects have been variously argued to be more consistent with one model or the other.[20,21] Key experimental results have also been interpreted as strongly indicative of one of the two types of defects, including two LESR studies on both sides of the argument. First, a report that the LESR signal gains intensity upon halogen doping[22] was suggestive that the photoinduced defect is charged, consistent with a polaron description. Second, a report that the LESR signal exhibits motional narrowing without a measurable increase in conductivity[11] was argued as incontrovertible evidence that the photoinduced defect is neutral, consistent with the soliton description. From our laboratory, characterization of a variety of photoinduced spectral signatures, including absorption,[23] resonance Raman[19] and LESR (Ref. 13) data, have generally been advanced within the polaron description. With regard to the LESR spectra from ^{15}N-labeled en, the number of the peaks and approximate intensities observed with 16-G spacing were suggested to originate from a polaron defect in which four equivalent Cl nuclei surround two partially oxidized or reduced Pt sites within the reduced or oxidized metal sublattice, respectively (two Pt sites with an intervening Pt, see Fig. 1).[13] Intuitively, however, the soliton model seems more reasonable in that the two Pt sites associated with the defect are adjacent. Furthermore, a soliton model based on *K*-band ESR results[15] provided an example of a simulation that is successful at reproducing the HF features at all angles. In our assessment, however, this model is not satisfactory in that it continues to associate the SHF structure with the nitrogen nuclei and also yields the prediction that 40% of the spin density in the defect is located on a single bridging chlorine nucleus, which is unexpected based on the similarity of the magnitude of the H-F splitting to LESR signals observed for stacked (bridgeless) Pt compounds.[24]

Clearly, understanding the SHF structure could greatly improve the prospects for accurate characterization of the defect responsible for the LESR signal. Part of the difficulty in clarifying the nature of the SHF features is due to the fact that they are distributed over the five-line Pt HF pattern, where they overlap and exhibit varying resolution. To clarify the nature of the defect and the HF/SHF interactions, samples of PtCl were prepared with enriched nuclear isotopes including ^{194}Pt ($I=0$), ^{2}H ($I=1$), and ^{37}Cl (like ^{35}Cl, $I=3/2$, but with a magnetogyric ratio $\sim$83% that of ^{35}Cl) and studied by LESR.

II. EXPERIMENT

(1) *Materials:* all isotopes were purchased from Oak Ridge National Laboratory. The ^{194}Pt was certified to have a ^{195}Pt concentration of less than 3%. The ^{37}Cl was purchased as NaCl. The samples of Pt-Cl were synthesized from the saturated aqueous perchloric acid solution of $[Pt^{II}(en)_2]^{2+}$ and $[Pt^{IV}(en)_2]^{4+}$ by the literature method[25] and recrystallized in the absence of light at around 5 °C to obtain single crystals of Pt-Cl, with a typical dimension of about $4\times2\times0.5$ mm^3. The crystals were stored below 15 °C.

(2) *ESR spectroscopy:* single crystals of Pt-Cl were taken from the aqueous solution, dried on tissue paper, and oriented on a quartz capillary by means of a small amount of vacuum grease prior to insertion into a 4 mm quartz tube with a stopcock. The sample tube was evacuated for several minutes prior to placement within the cavity of an IBM (Bruker) series ER 200 *X*-band spectrometer equipped with an Oxford liquid-helium cryostat. The sample was cooled to 10 K or below and a spectrum recorded. No significant signals were observed prior to irradiation. The sample was then irradiated for 1 h with a 50 mW/mm^2 Ar^+ laser beam operated in the visible all-lines mode. The spectra were then recorded at various temperatures from 4 to 300 K and at various orientations between the magnetic field and the primary crystal axis, which was identified as the chain axis by examination with an analyzer.

III. RESULTS

A. LESR studies of isotope-labeled Pt-Cl at 10 K

The LESR spectra of ^{194}Pt-^{N}Cl (N denotes natural abundance) were measured at various orientations as shown in Fig. 2. Compared with the well established LESR results[7,10] of ^{N}Pt-^{N}Cl, which exhibit the five-line pattern described above, the spectrum of ^{194}Pt-^{N}Cl at $g_\perp$, as expected, shows only a single line with peak-peak linewidth of $H_{pp}\sim90$ G. The spectrum from ^{194}Pt-^{N}Cl broadens when the orientation is changed from 90° to 0°, while the SHF features undergo extensive changes and are essentially unresolved or absent in the $g_\parallel$ spectrum. Figure 3 shows the comparative spectra of ^{N}Pt-^{N}Cl with deuterium-labeled en ligand groups, and ^{194}Pt-^{N}Cl with hydrogen-labeled en. The deuterated ^{N}Pt-^{N}Cl spectrum is essentially the same as that from ^{N}Pt-^{N}Cl synthesized with hydrogen,[7] demonstrating that the LESR spectrum is not influenced by the hydrogen nuclei. Having elimi-

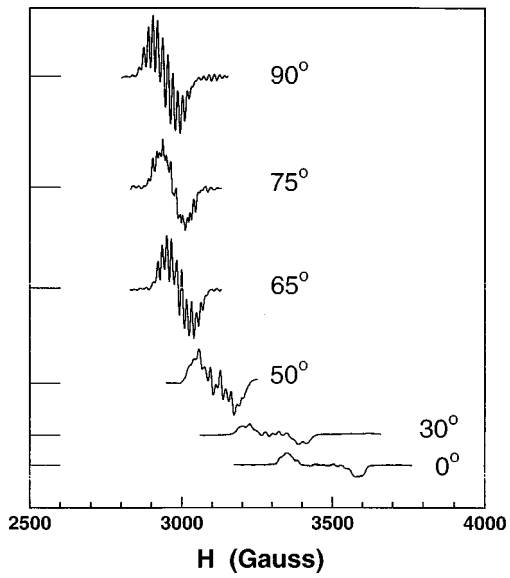

FIG. 2. The LESR spectra of ^{194}Pt-^{N}Cl at various orientations, where N denotes the element with natural abundance of isotopes. Data were acquired with temperatures around 6 K.

nated the possibilities that the SHF originates from hydrogen and nitrogen[13] (as well as the remote possibility that it is due to Pt), the SHF structure must indeed originate from the chlorines. This conclusion is tested by LESR experiments on ^{194}Pt-^{37}Cl.

Natural Cl consists of 75.77% ^{35}Cl and 24.23% ^{37}Cl with a ratio of magnetogyric ratios of $\gamma_{^{35}\mathrm{Cl}}/\gamma_{^{37}\mathrm{Cl}} \approx 1.20$. Thus, the relative ratio between the average magnetogyric moment of ^{N}Cl and that of ^{37}Cl is expected to be about 1.15. Figure 4 compares the integrated LESR spectra from ^{194}Pt-^{N}Cl with that from ^{194}Pt-^{37}Cl. The overall spectral width of ^{194}Pt-^{N}Cl is clearly broader than that of ^{194}Pt-^{37}Cl at both the perpendicular and parallel orientations, and we measure this broadening factor to be approximately 1.16. Moreover, the average SHF splitting also varies by the same ratio (15.8 G vs 13.6 G) for ^{194}Pt-^{N}Cl and ^{194}Pt-^{37}Cl at $g_{\perp}$. This result shows that (1) the SHF structure unequivocally originates from chlorines; (2) the overall spectrum is fundamentally comprised of a superposition of individual chlorine SHF lines. Regarding the inconsistency reported in the literature with respect to the

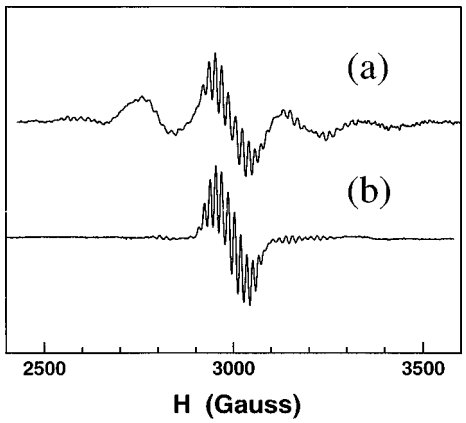

FIG. 3. The comparative spectra of (a) ^{N}Pt-^{N}Cl with deuterium-labeled en ligands, and (b) ^{194}Pt-^{N}Cl with hydrogen-labeled en.

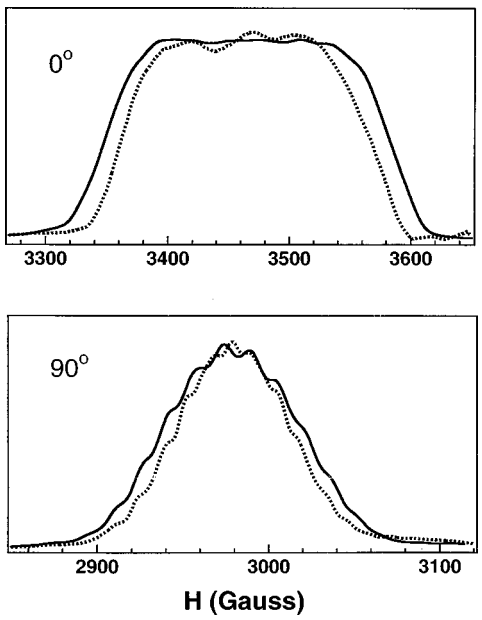

FIG. 4. The comparative LESR spectra of ^{194}Pt-^{N}Cl (solid lines) and ^{194}Pt-^{37}Cl (dashed lines) at $g_{\parallel}$ and $g_{\perp}$, respectively. The integrated ESR spectra are plotted here to emphasize the overall spectral width variations upon chlorine isotope substitution. The superhyperfine splitting is also seen to vary.

appearance of the SHF structure,[7,10–16] we conducted measurements on a variety of samples under identical experimental conditions and observed the linewidth of individual SHF lines to be quite sample dependent. In all cases, however, the SHF splitting remains unchanged, indicating that the SHF structure is affected by variations in spin-relaxation rates.

B. Spectral dependence on temperature, frequency, and microwave power

The temperature dependences of the ESR spectra of ^{N}Pt-^{N}Cl and ^{194}Pt-^{N}Cl are shown in Figs. 5(a) and 5(b), respectively. As expected, the LESR signal discussed to this point exhibits a rapid intensity decrease when the sample temperature is raised from 10 to around 200 K, where it is not discernable, and the spectrum is only partly recovered upon cooling. No motional narrowing or collapse of the ESR spectrum is observed at any temperature. This is the case for the $I_z = \pm 1/2$ lines shown for ^{N}Pt-^{N}Cl up to 140 K, and these lines are not observed above 170 K, which we consider to be the result of diminished signal to noise, rather than motional collapse. The central line is observed up to around 200 K, but exhibits no changes in line shape. For ^{194}Pt-^{N}Cl, as shown in Fig. 5(b), no changes are observed in the linewidth up to 200 K. Although the conclusion that no motional effects are observed in the ESR data is not in agreement with a previous report,[7,11] it is consistent with the idea that such localized solitons in strong CDW materials should be quite immobile.[26]

Surprisingly, we observed drastic changes in the LESR spectrum of ^{N}Pt-^{N}Cl from 10 to 4 K, as shown in Fig. 6. The spectrum at 10 K shows the ''normal'' 1:8:18:8:1 hyperfine intensity ratio and SHF structures. At 4 K, no SHF structure was observed under our normal measuring condition (modu-

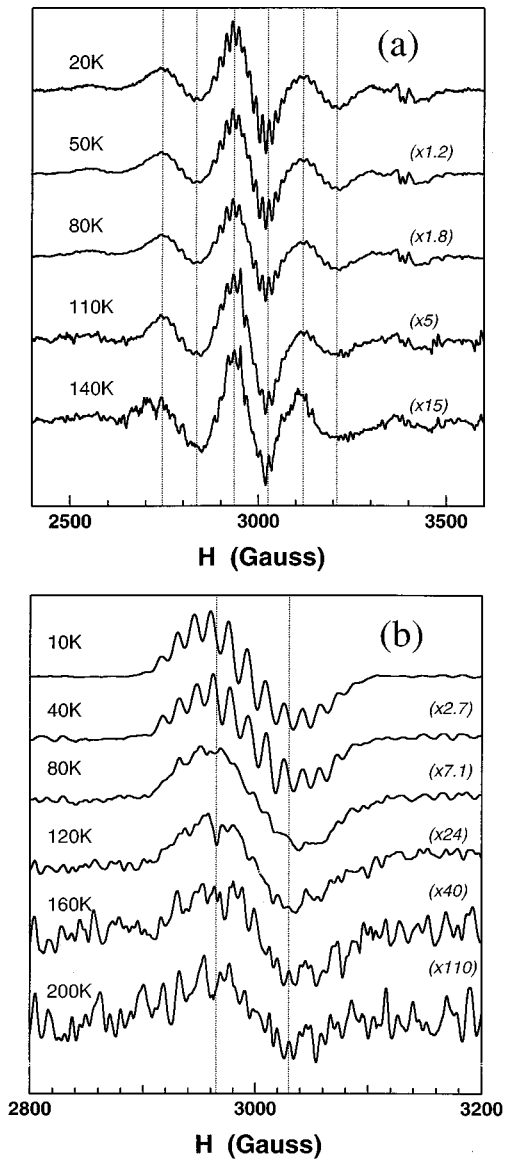

FIG. 5. Temperature dependence of the (a) ^{N}Pt-^{N}Cl and (b) ^{194}Pt-^{N}Cl LESR spectrum at $g_{\perp}$.

lation frequency and microwave power dependences are discussed below). The integrated intensity for the five HF lines at 4 K becomes $0.7:17.7:17:16.5:0.7\pm0.2$, where the intensity units of the 10 K spectrum are preserved. Note that the two $I_z=\pm1/2$ HF lines gain intensity dramatically (more than doubled), while the other three lines lose a relatively small amount of intensity from 10 to 4 K. Overall, the spectral intensity increases by nearly 50%. Moreover, the linewidths of the five HF lines change from an approximately uniform value of 108 G at temperatures above 6 K to 94, 184, 103, 184, 94 G at 4 K. Finally, the separation between the two $I_z=\pm1/2$ HF lines decreases from 360 to 260 G, while the other lines remain comparatively, but not perfectly (*vide infra*) fixed.

Because the ''normal'' 1:8:18:8:1 hyperfine intensity pattern in ^{N}Pt-^{N}Cl results from the probability of finding total nuclear-spin moment, I_z, of the two Pt at -1, $-1/2$, 0, 1/2, and 1, one might assume that deviation from this distribution is due to the sudden appearance of an unrelated defect which

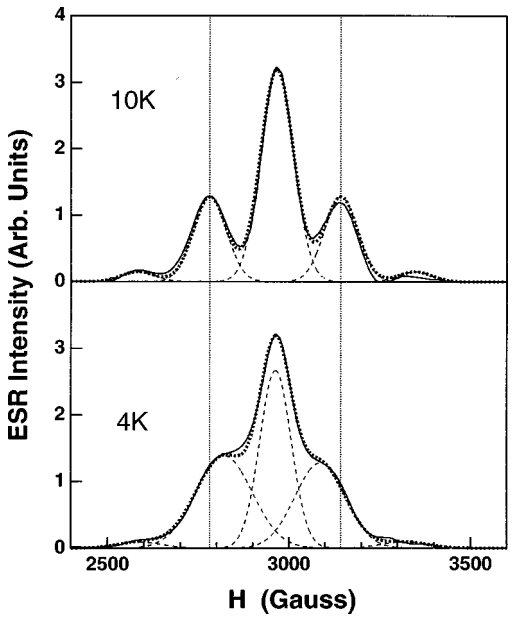

FIG. 6. Comparative ^{N}Pt-^{N}Cl LESR spectra at 4 and 10 K, respectively. The solid lines are experimental data, the dashed lines are the five Gaussian components for each temperature respectively, and the dotted lines are the resultant simulations.

contributes to the excess spectral weight.[16] Accordingly, the 4 K LESR spectrum of ^{194}Pt-^{N}Cl would be expected to reveal this new defect more cleanly because there is no interference from the $I_z=\pm1/2$ HF lines in ^{194}Pt-^{N}Cl. Figure 7 shows the low-temperature dependence of the ESR spectrum for ^{194}Pt-^{N}Cl. It is striking that there is no counterpart in the 4 K ^{194}Pt-^{N}Cl spectrum to the increased spectral weight in the analogous spectrum of ^{N}Pt-^{N}Cl. Thus, if such a ''new'' defect exists, it would be selectively localized on only the ^{195}Pt ($I=1/2$) sites and be totally absent in ^{194}Pt-^{N}Cl, which is extremely unlikely. Excess spectral features were also observed by Ota *et al.* However, there are several significant differences. (1) Our spectral alterations ''disappear'' above 6 K, while those of Ota *et al.* persist up to nearly 30 K. (2) The excess intensity in our data is unlike that observed by Ota *et al.* in that it reappears if the sample is recooled below 4 K. (3) Our result does not depend on whether the Pt-Cl crystal

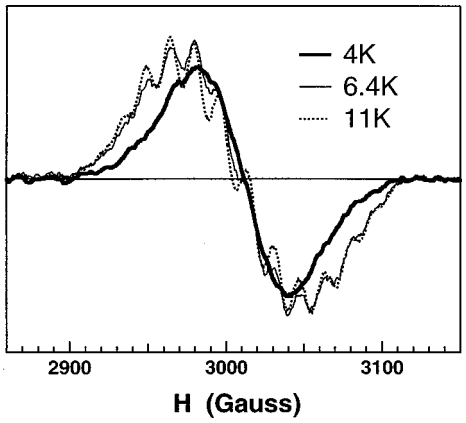

FIG. 7. Temperature dependence of the ^{194}Pt-^{N}Cl LESR spectrum at $g_{\perp}$. The spectrum undergoes dramatic changes from 4 to 6.4 K and stays relatively unchanged between 6.4 and 11 K.

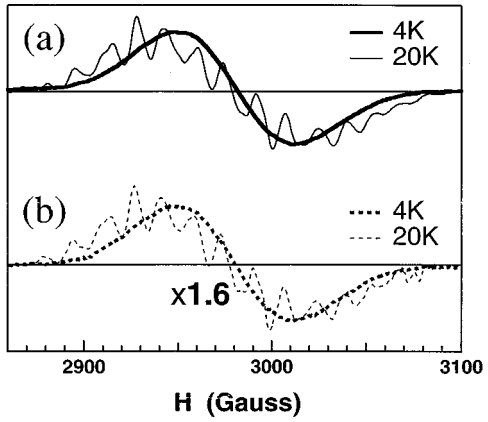

FIG. 8. LESR spectra at 4 and 20 K. The thick lines in (a) and (b) were obtained at 4 K while the thin lines were obtained at 20 K. The two panels reveal the relative intensities of the spectra taken at the two temperatures before (a) and after (b) temperature cycling.

has been through the monoclinic to orthorhombic phase transition. (4) We did not observe any photosaturation effect on the excess weight.

Figure 7 also shows that the SHF structure is largely suppressed at 4 K and appears quite suddenly when the temperature is raised from 4 to only 6 K. In fact, the spectrum at 4 K is distinct from that at 6 K in several ways. Quite unexpected is the observation that the bandwidth is more narrow by $\sim$17 G at 4 K. In addition, there is a slight shift ($\Delta g \sim 0.001$) of the spectrum. In comparison, the spectral profile remains relatively unchanged from 6 to 70 K. The rapid change in the overall width and g value of the ^{194}Pt-^{N}Cl LESR spectrum at low temperatures is consistent with the ^{N}Pt-^{N}Cl results where the central HF line corresponding to $I_z=0$ also narrows and shifts at 4 K (Fig. 6). To again consider the possibility that these two spectra represent the presence of unrelated defects, i.e., the spectrum at 4 K represents one defect and the excess spectral weight in the 6 K spectrum represents another, we studied the LESR spectrum after temperature cycling between 4 K and higher temperatures (near 80 K). Figure 8 shows the comparative LESR spectra at 4 and 20 K before [Fig. 8(a)] and after [Fig. 8(b)] temperature cycling. The thick line spectra in Figs. 8(a) and 8(b) were taken at 4 K, while the thin curves were obtained at 20 K. Although Fig. 8(b) reveals that the intensity is decreased by more than 35% after the temperature cycles, the 4 and 20 K spectra in the two parts of the figure retain the same relative intensities. The possibility that two defects with superimposed spectra experience identical annihilation with raised temperatures is not credible. Thus, the spectral variations between 4 and 6 K are associated with a single type of defect.

We also found that variations of the modulation frequency and microwave power at 4 K affect the spectrum in a manner similar to raising the temperature to 6 K. In ^{194}Pt-^{N}Cl, where the SHF lines are not resolved at 4 K under typical measurement conditions (modulation frequency=100 kHz; microwave power=2–20 mW), the structure becomes well resolved when measured at low modulation frequency (for example, 3 kHz) and/or reduced microwave power (for example, 2 μW). Figure 9 shows the integrated 4 K LESR spectra of ^{194}Pt-^{N}Cl measured at field modulation frequency of 100 and 3 kHz, respectively. Similarly, the spectrum of

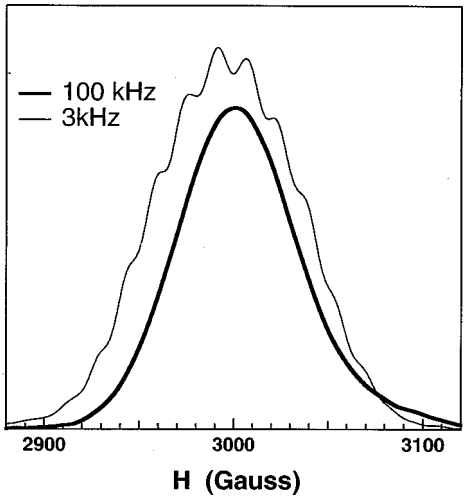

FIG. 9. The comparative LESR spectra of ^{194}Pt-^{N}Cl measured with field modulation frequencies of 100 and 3 kHz.

^{N}Pt-^{N}Cl measured at low microwave power shows that the two $I_z=\pm 1/2$ HF lines are less broadened as compared with the spectrum measured at high microwave power. This could be an indication that the spin-lattice relaxation time, T_1, decreases rapidly when the temperature is raised above 4 K, and that microwave saturation effects are responsible for the spectral changes. However, the fact that the $I_z=\pm 1/2$ lines alone lose significant intensity above 4 K, while the other lines behave in the opposite manner is not consistent with this idea. Finally, the fact that the 6 K spectral profile can be recovered at 4 K by variations in the instrumentation settings does not suggest that the fundamental defect structure has been altered by a phase transition.

C. Sample-dependent defects

In addition to the LESR signatures presented so far, which were found for all samples, we also observed two other defects which exhibit extensive sample-to-sample variability. One defect is shown in Fig. 10, where two Gaussian-shaped satellite lines separated by 750 G are observed with sample-

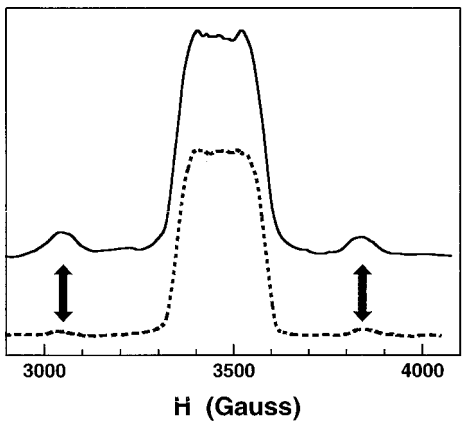

FIG. 10. The sample-dependent triplet exciton spectrum. The solid and dashed lines represent integrated LESR spectra for two different samples. The arrows point to the field positions of the triplet exciton magnetic resonance.

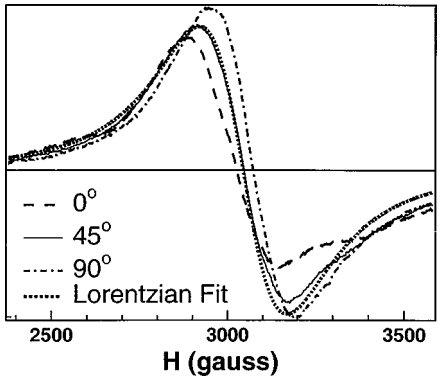

FIG. 11. ESR spectra of the sample-dependent metastable defects at room temperature.

dependent intensity compared with the typical LESR spectrum at $g=1.95$. Because they have a much narrower width than the central line, these two lines cannot be attributed to a ^{195}Pt impurity, in which case the satellite lines should have the same width as the central line. Furthermore, any ^{195}Pt impurity would not be expected to show sample to sample variations, since the samples were crystallized from a single synthetic preparation. These two peripheral bands were occasionally observed both in ^{194}Pt-^{N}Cl prepared with ^{2}H-substituted en ligands as well as the normal en samples; thus, they are not from hydrogen-related defects. Moreover, if these two lines were due to the hyperfine interactions between the unpaired spin and some unknown nuclear spin-1/2 site, the separation of 750 G would lead to a hyperfine coupling constant of 1500 G, which is about as large as that of free hydrogen atoms, i.e., the unpaired spin would be completely localized on a hydrogen 1s orbital. We tentatively attribute the separation of 750 G to the zero-field splitting of a triplet exciton. Half-field resonance signals have not been observed, although these would be expected to be quite weak in an X-band ESR measurement. The irregular observation of this defect could be a contributor to the inconsistency of the $g_{\|}$ spectra reported in the literature.

The second type of sporadic LESR signal, shown in Fig. 11, was observed at temperatures above 120 K. Unlike the lower temperature signal, this ESR signal exhibits intensity increases when the temperature is raised, presumably due to more rapid spin-lattice relaxation at higher temperatures (this assumption was not tested by investigation of power saturation effects at lower temperatures). This LESR signal is very intense at room temperatures and can persist after several days at room temperature, much longer than the room-temperature lifetime of the photoinduced defects observed at low temperatures. This new metastable defect has a comparatively isotropic g tensor with $g_{\|}=2.26$ and $g_{\perp}=2.23$ and with $\Delta H_{pp}\sim 150$ G. Note also that $g_{\|}>g_{\perp}$, in contrast with $g_{\|}<g_{\perp}$ for the primary low-temperature signal. We suggest that the disagreement between the present study and that from Kuroda *et al.* regarding the observation of motional narrowing is due to the presence of this signal in their data. That study shows the fully separated HF bands up to 60 K and a broadband above 200 K (see Fig. 4 in Ref. 11). Furthermore, in our opinion the spectra recorded at 160 and 180 K in that report do not definitively reveal a collapse of the HF structure. In fact, despite the poor signal-to-noise associated with LESR spectra at those temperatures, evidence of the $I_z=\pm 1/2$ lines at their original low-temperature positions without collapse is observed. In the present case, the broader linewidth of the metastable signal ($\sim$150 G) from ^{194}Pt-Cl excludes the possibility of motional narrowing associated with the low-temperature spectrum ($H_{pp}\sim 90$ G). The origin of this metastable defect is not clear at present. It may be related to the long-lived photoinduced absorption bands reported previously for Pt-Cl.[27]

IV. DISCUSSION

A. Primary photoexcitations in Pt-Cl

The LESR spectrum in Pt-Cl has been assigned both to polarons and solitons. The $g_{\perp}$ ESR spectrum can be approximately reproduced by both polaron and soliton-spin distributions such as those illustrated in Fig. 1. However, there has been no model of the ESR data that convincingly mimics the spectrum at all angular orientations. One polaron model[13] predicts that four equivalent (excepting isotope) Cl nuclei contribute to the SHF structure, whereas a simple soliton model[15] predicts that one Cl nucleus is strongly coupled to the spin. Both defect models are explored here in an attempt to simulate the ^{194}Pt-^{N}Cl LESR spectra observed at all angles. Unlike the previous soliton model, however, our simulation includes three chlorines, two of which are equivalent and lie at the periphery of the defect and one of which is centralized and more strongly coupled to the spin. Thus, the following Hamiltonian was used for the spin-soliton simulation:

$$\mathcal{H}=\beta\mathbf{S}\cdot\overleftrightarrow{g}\cdot\mathbf{H}+\mathbf{S}\cdot\overleftrightarrow{A}_{\mathrm{Cl}_c}\cdot\mathbf{I}_{\mathrm{Cl}_c}+\sum_{i=1}^{2}\mathbf{S}\cdot\overleftrightarrow{A}_{\mathrm{Cl}_o}\cdot\mathbf{I}_{\mathrm{Cl}_o}, \qquad (1)$$

where $\overleftrightarrow{A}_{\mathrm{Cl}_c}$ denotes the hyperfine tensor for the central Cl site, while $\overleftrightarrow{A}_{\mathrm{Cl}_0}$ denotes that of the outer Cl sites. The simulated spectra were calculated assuming random distribution of Cl isotopes in accord with natural abundance. For the polaron simulation, the following spin Hamiltonian was used:

TABLE I. Parameters used in the soliton model.

$g_{\|}=1.943$	$g_{\perp}=2.293$
$A_{\|}c=47\times10^{-4}$ cm^{-1} (for ^{35}Cl)	$A_{\perp}c=28\times10^{-4}$ cm^{-1} (for ^{37}Cl)
$A_{\|}c=39\times10^{-4}$ cm^{-1} (for ^{37}Cl)	$A_{\perp}c=23\times10^{-4}$ cm^{-1} (for ^{37}Cl)
$A_{\|}o=11\times10^{-4}$ cm^{-1} (for ^{35}Cl)	$A_{\perp}o=14\times10^{-4}$ cm^{-1} (for ^{35}Cl)
$A_{\|}o=9.3\times10^{-4}$ cm^{-1} (for ^{37}Cl)	$A_{\perp}o=11\times10^{-4}$ cm^{-1} (for ^{37}Cl)

TABLE II. Parameters used in the polaron model.

$g_{\parallel}=1.943$	$g_{\perp}=2.293$
$A_{\parallel}=35.00\times10^{-4}$ cm^{-1} (for ^{35}Cl)	$A_{\perp}=14.96\times10^{-4}$ cm^{-1} (for ^{35}Cl)
$A_{\parallel}=29.12\times10^{-4}$ cm^{-1} (for ^{37}Cl)	$A_{\perp}=12.45\times10^{-4}$ cm^{-1} (for ^{37}Cl)

$$\mathcal{H}=\beta\mathbf{S}\cdot\overleftrightarrow{g}\cdot\mathbf{H}+\sum_{i=1}^{4}\mathbf{S}\cdot\overleftrightarrow{A}_{\mathrm{Cl}}\cdot\mathbf{I}_{\mathrm{Cl}}. \tag{2}$$

The optimum parameters (by visual inspection of the simulated result) from the two simulations are listed in Tables I and II.

Figure 12 shows the simulation of LESR spectra of ^{194}Pt-^{N}Cl based on the two models compared with the data acquired for that orientation. Examination of the calculated spectra for the two extreme and one intermediate angles reveals that the spin-soliton model gives a better overall fit to the LESR data. The equivalency of Cl nuclear sites in the polaron model entails binomial distribution of the SHF lines,[28] which tends to have higher (integrated) ESR intensity and larger SHF line amplitude in the middle of the spectra. The soliton model permits adjustment of the electron-spin density on the two types of Cl sites, thereby allowing a superior fit of the spectra. The model is successful in that it reproduces the principle features of the data at all angles, including the resolved SHF in $g_{\perp}$ and the tripletlike appearance of $g_{\parallel}$, where the contribution of the bridging chlorines is more extensive yet the resolution of the SHF is lost. The polaron model is especially poor at reproducing this featureless signal. Using an argument similar to that proposed by Kuroda *et al.*,[15] the unpaired electron is estimated to have 15% density on the p_z orbit of the central Cl site and 2% on each of the outer Cl^{-} sites. These values differ markedly from a previously proposed model in which 40% of the spin density was found on the bridging chlorines.[15]

While the present soliton model is generally accurate at all angles, some details are not reproduced. Perhaps most important is the inability to yield good registry with the SHF features of the $g_{\perp}$ spectrum, as seen by careful inspection of Fig. 12. The simulated intensity pattern is also not a good match to the data, in that excess intensity is predicted for the bands at the edge of the spectrum. Such discrepancies could be due to the simplified nature of the model Hamiltonian, which includes the assumption that the principal axes of the g and A tensors are coincident. The differences could also partly be a result of the presence of heterogeneous defect structures. Such are indicated by sample to sample variability in the relative intensities of the SHF features and the fact that the individual SHF bands often exhibit structure (see Fig. 8) which is not reproduced by the model. One previous result that supports such a possibility is the observation of multiple pinning energies for photoinduced spin defects in the bromine analog of Pt-Cl, Pt-Br.[29]

B. Possibility of spin dynamics at 4 K

The spectral changes of the HF structure, which is associated with Pt nuclei, and the SHF structure, which is associated with Cl nuclei, at low temperatures are quite unusual. The intensity pattern of 0.7:17.7:17:16.5:0.7 (±0.2) at 4 K is especially puzzling because no obvious configuration can yield such an intensity pattern in accord with the statistical distribution of the Pt isotopes. Yet in Sec. III B, we concluded that these changes are unlikely to be due to the emergence of new defects, phase transitions, or saturation effects. Therefore, the spectral changes observed between 4 and 6 K are apparently a manifestation of a dynamic process. Because the intensities of the LESR spectra observed upon cycling between 4 and 6 K are reproducible, any dynamics are apparently localized and do not lead to activation or annihilation of the defect. Sakai *et al.*[14] proposed a dynamical model to explain the observation in ^{N}Pt-^{N}Cl that the SHF lines are present in the $I_z=0$ and ±1 HF lines and absent in the $I_z=\pm1/2$ HF lines. In their model, the spin density of neutral solitons are fluctuating back and forth around the equilibrium position. However, in such an instance one would also expect the overall linewidths of the two $I_z=\pm1/2$ lines to be broader than the other three HF lines, which is not in agreement with the LESR spectra at temperatures higher than 6 K. Below 6 K, the two $I_z=\pm1/2$ lines do indeed broaden and collapse toward the central $I_z=0$ line from 6 to 4 K. In this instance, the classical Anderson spin-exchange narrowing model can be investigated for applicability:

$$[\Delta H_{12}(0)]^2-(\Delta H_{12})^2=2(\Gamma-\Gamma_0)^2, \tag{3}$$

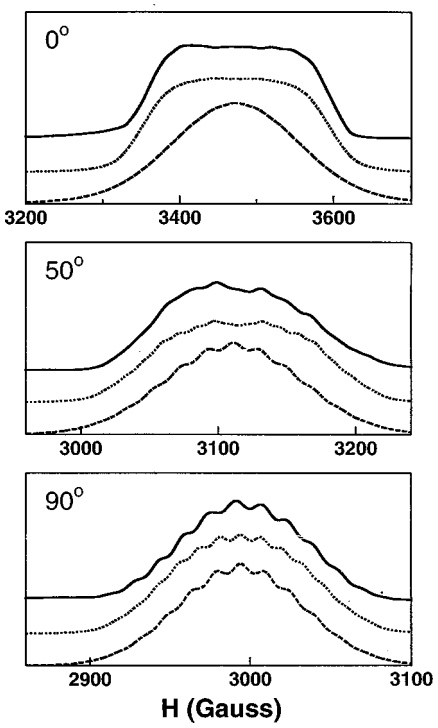

FIG. 12. The experimental (solid lines) and simulated ESR spectra based on neutral soliton (dotted lines) and polaron (dashed lines) models at a variety of angles.

where the resonant lines are at fields H_1 or H_2 with $\Delta H_{12} = H_2 - H_1$, Γ_0 is the intrinsic linewidth, Γ is the measured linewidth and $\Delta H_{12}(0)$ is the intrinsic splitting without spin exchange. However, the values extracted from Fig. 6, i.e., $\Delta H_{12}(0) = 360$ G, $\Delta H_{12} = 270$ G, $\Gamma_0 = 108$ G, and $\Gamma = 184$ G, are not in accord with Eq. (3). In general, any simple dynamical model is not likely to explain the low-temperature phenomenon in Pt-Cl. In fact, the data provide a surprising indication that the dynamic phenomenon is not evenly applied among the isotopically distinct defect sites. Because it is well established that quantum lattice fluctuations affect both the electronic properties of the ground and photoinduced states, we speculate that low-frequency internal modes, apparently on time scales similar to the modulation frequency of the ESR measurement, couple to the spin dynamics.

V. CONCLUSIONS

We have measured the LESR spectra of various isotopically enriched Pt-Cl complexes. These results show that the superhyperfine (SHF) structures are purely associated with Cl and the spin-1/2 defects can be better modeled as neutral solitons by a simple Hamiltonian including significant spin density over three Cl sites. This result is in opposition to our earlier assignment of the LESR spectrum to polarons and is accord with the general assignment from Kuroda and coworkers, although our results call several aspects of their soliton model into question. As one example, we can find no indication of motional narrowing of the LESR spectrum. A redistribution of spectral intensities below 6 K is believed to result from some unusual spin dynamics in Pt-Cl. These dynamics are not easily understood and appear to be sensitive to isotope. Two sample-dependent defect signatures were observed, one of which appears to be a spin triplet, while another appears above 120 K and is metastable at room temperature. Thus, it is clear that a variety of spin photoexcitations are possible for Pt-Cl, although the soliton result seems to be common to all instances.

ACKNOWLEDGMENTS

We gratefully acknowledge the insight and suggestions provided by Professor David F. Bocian. We would also like to thank Drs. A. R. Bishop, A. Saxena, and J. T. Gammel for useful discussions. Work at LANL was supported by the Laboratory Directed Research and Development fund.

*Author to whom correspondence should be addressed.

[1] H. J. Keller, in *Extended Linear Chain Compounds*, edited by J. S. Miller (Plenum, New York, 1983), Vol. 1, p. 357.
[2] N. Kuroda, M. Sakai, Y. Nishima, M. Tanaka, and S. Kurita, Phys. Rev. Lett. **58**, 2122 (1987).
[3] H. Okamoto, T. Mitani, K. Toriumi, and M. Yamashita, Phys. Rev. Lett. **69**, 2248 (1992).
[4] R. J. H. Clark, in *Advances in Infrared and Raman Spectroscopy*, edited by R. J. H. Clark and R. E. Hester (Wiley Heyden, New York, 1984), Vol. 11, p. 95, and references therein.
[5] L. DeGiorgi, P. Wachter, M. Haruki, and S. Kurita, Phys. Rev. B **40**, 3285 (1989); **42**, 4341 (1990).
[6] T. Kobayashi, H. Ooi, and M. Yamashita, Mol. Cryst. Liq. Cryst. Sci. Technol., Sect. A **256**, 847 (1994).
[7] A. Kawamori, R. Aoki, and M. Yamashita, J. Phys. C **18**, 5487 (1985).
[8] A. Mishima and K. Nasu, Phys. Rev. B **39**, 5758 (1989); **39**, 5763 (1989).
[9] J. T. Gammel, A. Saxena, I. Batistic, A. R. Bishop, and S. R. Phillpot, Phys. Rev. B **45**, 6408 (1992); S. M. Weber-Milbrodt, J. T. Gammel, A. R. Bishop, and E. Y. Loh, *ibid.* **45**, 6435 (1992).
[10] S. Kurita and M. Haruki, Synth. Met. **29**, F129 (1989).
[11] N. Kuroda, M. Sakai, M. Suezawa, Y. Nishina, and K. Sumino, J. Phys. Soc. Jpn. **59**, 3049 (1990).
[12] N. Kuroda, M. Sakai, M. Suezawa, Y. Nishina, K. Sumino, and M. Yamashita, Mol. Cryst. Liq. Cryst. Sci. Technol., Sect. A **216**, 169 (1992).
[13] C. A. Arrington, C. J. Unkefer, R. J. Donohoe, S. C. Huckett, S. Kurita, and B. I. Swanson, Solid State Commun. **84**, 979 (1992).
[14] M. Sakai, N. Kuroda, M. Suezawa, Y. Nishina, K. Sumino, and M. Yamashita, J. Phys. Soc. Jpn. **61**, 1326 (1992).
[15] N. Kuroda, M. Ito, Y. Nishina, A. Kawamori, Y. Kodera, and T. Matsukawa, Phys. Rev. B **48**, 4245 (1993).
[16] S. Ota and S. Kurita, Mol. Cryst. Liq. Cryst. Sci. Technol., Sect. A **256**, 879 (1994).
[17] S. Kurita, M. Haruki, and K. Miyagawa, J. Phys. Soc. Jpn. **57**, 1789 (1988).
[18] N. Kuroda, M. Nishida, and M. Yamashita, Phys. Rev. B **52**, 17 084 (1995). This study is of the BF_4 analog of the ClO_4Pt-Cl complex.
[19] R. J. Donohoe, C. D. Tait, and B. I. Swanson, Chem. Mater. **2**, 315 (1990).
[20] J. T. Gammel, R. J. Donohoe, A. R. Bishop, and B. I. Swanson, Phys. Rev. B **42**, 10 566 (1990).
[21] N. Kuroda, M. Kataoka, and Y. Nishina, Phys. Rev. B **44**, 13 260 (1991).
[22] M. Haruki and S. Kurita, Phys. Rev. B **39**, 5706 (1989).
[23] R. J. Donohoe, S. A. Ekberg, C. D. Tait, and B. I. Swanson, Solid State Commun. **71**, 49 (1989).
[24] T. Krigas and M. T. Rogers, J. Chem. Phys. **55**, 3035 (1971).
[25] S. C. Huckett, R. J. Donohoe, L. A. Worl, A. D. F. Bulou, C. J. Burns, J. R. Laia, D. Carrol, and B. I. Swanson, Chem. Mater. **3**, 123 (1991).
[26] Y. Onodera, J. Phys. Soc. Jpn. **56**, 250 (1987).
[27] G. Kanner, G. Strouse, and B. I. Swanson (unpublished).
[28] N. M. Atherton, *Principles of Electron Spin Resonance* (Ellis Horwood and Prentice Hall, Princeton, NJ, 1993).
[29] R. J. Donohoe, L. A. Worl, C. A. Arrington, A. Bulou, and B. I. Swanson, Phys. Rev. B **45**, 13 185 (1992).